CHEMISTRY
A EUROPEAN JOURNAL

DOI: 10.1002/chem.200700754

Controlled Synthesis, Growth Mechanism, and Properties of Monodisperse CdS Colloidal Spheres

Xin-Hao Li, Ji-Xue Li, Guo-Dong Li, Da-Peng Liu, and Jie-Sheng Chen*[a]

Abstract: Highly monodisperse submicrometer CdS colloidal spheres (CSCS) with a controllable and tunable size (between 80 and 500 nm) have been synthesized through a facile solvothermal technique. Owing to the controllability of the reaction process, the growth mechanism of the colloidal spheres has been elucidated in detail. The whole growth process can be summarized as homogenous and slow nucleation of nanocrystals, formation of "cores" through 3D-oriented attachment of nanocrystals, and further surface-induced growth to monodisperse colloidal spheres through in situ formation and random attachment of additional nanocrystals. It has been demonstrated that the obtained CSCS colloidal particles are able to be assembled into films which show characteristic stop band gaps of photonic crystals. By using the CSCS as a template, Ag_2S, Bi_2S_3, Cu_2S, HgS, and Sb_2S_3 colloidal spheres, which are difficult to obtain directly, have also been prepared successfully through ion exchange.

Keywords: cadmium · colloids · metal sulfides · nanoparticles · semiconductors

Introduction

Highly monodisperse colloidal particles have been intensively pursued as a result of their paramount importance in basic research and their practical applications.[1–5] Among the colloidal particles, those with a diameter in the submicrometer scale are of particular interest because they may be used as building blocks for self-assembly into 2D or 3D photonic crystals.[6–11] The optical properties of a photonic crystal are highly dependent on the refractive index of the spherical building blocks that form the photonic crystal, and an energy range, in which light can be neither emitted nor propagated, should exist if the refractive contrast between the building blocks and air (refractive index ≈ 1.0) is high enough. Nevertheless, so far only a few types of colloidal spheres, such as polymer and silica spheres, the refractive indices of which are usually lower than 1.6, have been exploited for photonic crystal applications owing to their convenience in large-scale preparation and in control of morphology.[12]

Highly monodisperse colloidal spheres of metal sulfides with relatively high refractive indices and unique physicochemical properties should be ideal building blocks for formation of photonic crystals with a wide band gap.[12,13] These colloidal spheres can also be applied in various areas, such as catalysis, ceramics, foams, pigments, and sensor fabrication.[14–17] Due to the importance of these spheres in various applications, there have been studies on synthetic approaches for monodisperse CdS or other metal-sulfide colloidal spheres. Several techniques,[18–27] including homogeneous deposition (or nucleation) and "gel–sol" techniques, have been successfully developed to obtain uniform CdS and ZnS colloidal spheres. For example, uniform CdS and ZnS colloidal spheres have been prepared[18–22] from diluted solutions of metal salts with thioacetamide (TAA) in an acidic system. Sugimoto and co-workers[23] further improved the homogeneous deposition method for a relatively larger scale synthesis of metal-sulfide colloidal spheres from concentrated solutions by introducing gelatin and proper chelating reagents. For these synthetic approaches, precise control of the reaction temperature was necessary and the synthetic conditions were restrictive. In order to meet the requirements for practical applications, the development of a facile, but effective approach for preparing high-quality metal sulfide colloidal spheres in copious quantities is highly desired.

[a] X.-H. Li, Prof. J.-X. Li, Prof. G.-D. Li, D.-P. Liu, Prof. J.-S. Chen
State Key Laboratory of Inorganic Synthesis and
Preparative Chemistry, College of Chemistry
Jilin University, Changchun 130012
People's Republic of China
Fax: (+86) 431-8516-8624
E-mail: chemcj@jlu.edu.cn

Supporting information for this article is available on the WWW under http://www.chemeurj.org/ or from the author.

WILEY InterScience DISCOVER SOMETHING GREAT
© 2007 Wiley-VCH Verlag GmbH & Co. KGaA, Weinheim

Meanwhile, highly uniform colloidal spheres of sulfides of metals other than Zn and Cd are difficult to prepare directly. Coating colloidal spheres[4,12,24] of silica or polymer (e.g. polystyrene), which acts as a template, is a feasible strategy for the preparation of non-zinc (cadmium) metal-sulfide colloidal spheres. However, the template-directed approach is complicated and the covering of the surface is usually poor. In general, this technique is unable to meet the requirements of various applications.

Herein, we demonstrate a solvothermal technique for the synthesis of highly monodisperse cadmium sulfide colloidal spheres (CSCS). In this solvothermal system, the size of uniform CSCS can be tuned continuously from the nanometer to the submicrometer scale by varying the reaction conditions. Precise control of the pH value, purity of the sulfur sources, and reaction temperature are not needed, neither a chelating agent. Furthermore, this method can be scaled up conveniently. By using a simple ion-exchange reaction, a series of uniform metal-sulfide spheres including Ag_2S, Bi_2S_3, Cu_2S, HgS, and Sb_2S_3 with spherical, hollow, or core/shell structures have been obtained. More importantly, our controllable reaction system provides a convenient experimental platform for gaining insights into the growth mechanism of the colloidal spheres at the nanometer level.

Results and Discussion

General characterization of monodisperse CSCS: The composition and morphology of the as-synthesized CSCS were elucidated first. The XRD pattern (Figure 1) for CSCS indicates that the product has a wurtzite structure (JCPDS 80-0006). The thermogravimetric and differential thermal analyses (TG-DTA, Figure S1a in the Supporting Information) reveal the presence of about 8 wt.% PVP (PVP = polyvinyl pyrrolidone) in the CSCS, although the CSCS sample had been thoroughly washed three times with deionized water before characterization. The presence of PVP in the CSCS is further confirmed by IR spectroscopy (Figure S1b, Supporting Information).

Figure 2 shows the SEM images of representative samples of uniform CSCS with different sizes; these images reveal the uniformity of spherical particles with a narrow size distribution. The respective size and size distribution (shown in Figure 3) were calculated by using the computer program Microcal Origin.

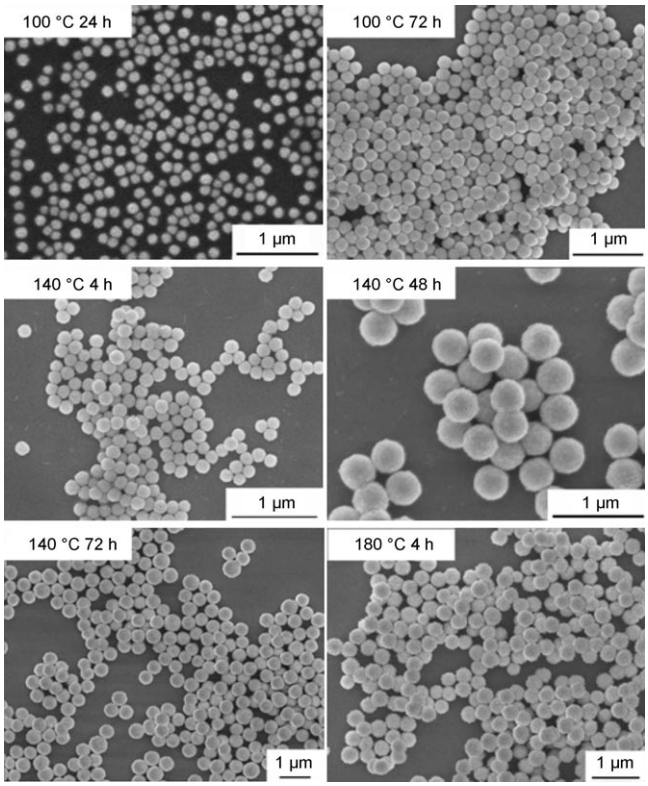

Figure 2. Typical SEM images of CSCS prepared under various reaction conditions (Cd^{2+}, TU, and PVP concentrations: 0.1 M each).

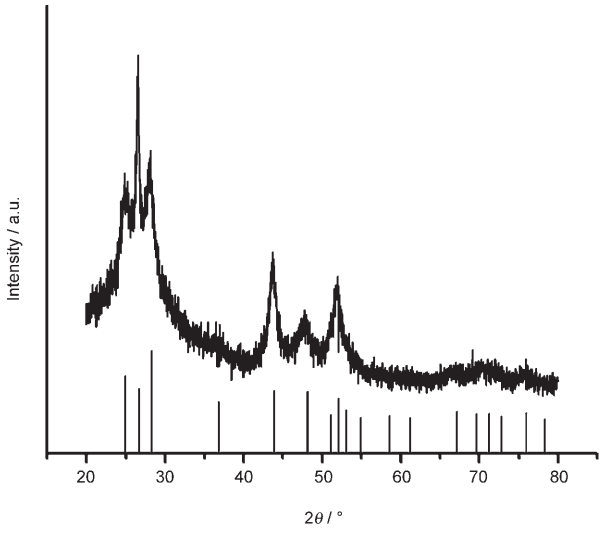

Figure 1. Typical powder XRD pattern of CSCS synthesized at 140 °C for 8 h (concentrations of Cd^{2+}, TU, and PVP are all 0.1 M). Bar: JCPDS 80–0006.

Factors influencing the formation of CSCS: Thiourea (TU), a sulfur source which has been commonly used for the deposition of metal-sulfide films[28,29] or other nanostructures in basic solutions,[30–32] remains stable up to 180 °C in reaction systems without metal cations. However, this compound decomposes at relatively low temperatures in an aqueous solution in the presence of many metal cations including Cd^{2+}. In our solvothermal system, a simple experiment was designed to demonstrate that the decomposition of TU is triggered by Cd^{2+} (Supporting Information, Figure S2) when the reaction temperature is lower than 180 °C. The slow, but continuous temperature-dependent decomposition of TU enables us to control the growth of CSCS by tuning the reaction conditions.

 © 2007 Wiley-VCH Verlag GmbH & Co. KGaA, Weinheim

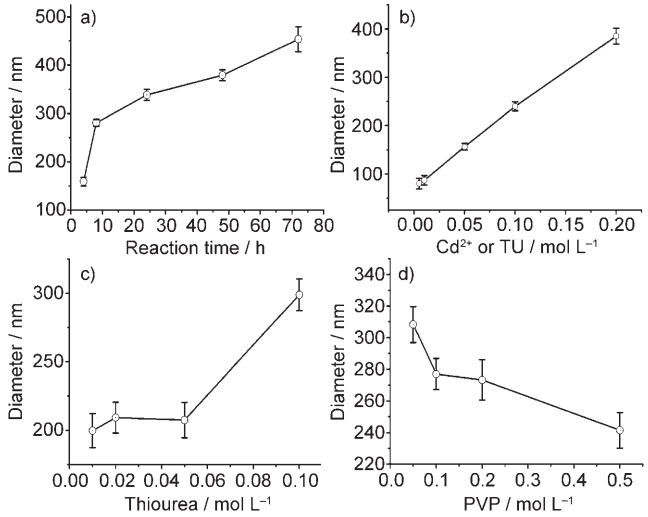

Figure 3. Plots of CSCS size and size distribution (represented by Y error bars) versus: a) Reaction time (Cd^{2+}, TU, and PVP concentrations: 0.1 M each, reaction temperature: 140 °C); b) Cd^{2+} or TU (Cd^{2+}/TU = 1:1) concentration (PVP concentration: 0.2 M, reaction temperature: 140 °C, reaction time: 8 h); c) TU concentration (Cd^{2+} concentration: 0.1 M, PVP concentration: 0.2 M, reaction temperature: 140 °C, reaction time: 10 h); and d) PVP concentration (Cd^{2+} and TU concentrations: 0.1 M each, reaction temperature: 140 °C, reaction time: 8 h).

As shown in Figures 2 and S3 (Supporting Information), reaction temperature affects the decomposition rate of TU, and as a result, it governs the nucleation and growth of CSCS. The time for the formation of monodisperse CSCS decreases as the temperature is increased. However, too high a temperature is not suitable for the formation of monodisperse CSCS from our reaction system, whereas too low a temperature takes too long to produce the monodisperse CSCS particles. Only at proper temperatures can the monodisperse CSCS with a continuously tunable size be prepared conveniently and efficiently. Furthermore, the surface smoothness of the CSCS is also affected by the reaction temperature. As illustrated in Figures 2 and S3–4 (Supporting Information), the surface of CSCS is smoother if the sample is prepared at 100 °C, and it becomes rougher when the reaction temperature is elevated to 180 °C. This is because at high reaction temperatures, the particle growth rate is too high for the primary units to stack in a gentle and smooth manner, whereas at lower temperatures, the stacking of primary units to form colloidal particles proceeds slowly and continuously.

Figure 3a shows a typical curve of particle size versus reaction time. Especially from 4 to 24 h, there is a relatively fast growth process. Afterwards, the growth rate decreases gradually as the TU is used up. In general, the colloidal particle size increases with reaction time. By varying the concentrations of the reaction reagents in a certain range, the size of uniform CSCS can be tuned conveniently, as shown in Figure 3b–d and S5–7 (Supporting Information), respectively. Only polydisperse spheres or irregular particles can be obtained from the reaction system when the concentration of Cd source (or TU) is larger than 0.5 M, or the concentration of PVP is not correct (that is, not in the range from 0.05 to 1 M). It is worth noting that the particle size increases linearly from 80 ± 10 to 385 ± 17 nm with variation of the concentrations of Cd source and TU (Cd/TU = 1:1), as shown in Figure 3b. The PVP molecules play an important role in preventing the spheres from agglomerating as many polymer molecules do in the formation of other spherical species.[12,33] However, when we used non-PVP surfactants, such as poly(ethylene glycol), poly(vinyl alcohol), poly(ethylene glycol)-*block*-poly(propylene glycol)-*block*-poly(ethylene glycol) for the preparation of CSCS, no spherical structures were obtained under the same reaction conditions. This observation suggests that the PVP molecules may be unique for the formation of the CSCS in the current reaction system.

It has been proven that our solvothermal method is scalable for the preparation of CSCS. For example, we successfully leveled up the typical synthesis of uniform CSCS ten times, by dissolving 10.797 g $Cd(NO_3)_2 \cdot 3H_2O$, 2.664 g TU, and 3.885 g PVP in 350 mL ethylene glycol and heating this solution at 140 °C for 10 h. After centrifugation and washing three times, we obtained 5.17 g of a yellow powder of uniform CSCS. From Figure 4, it is seen that highly uniform

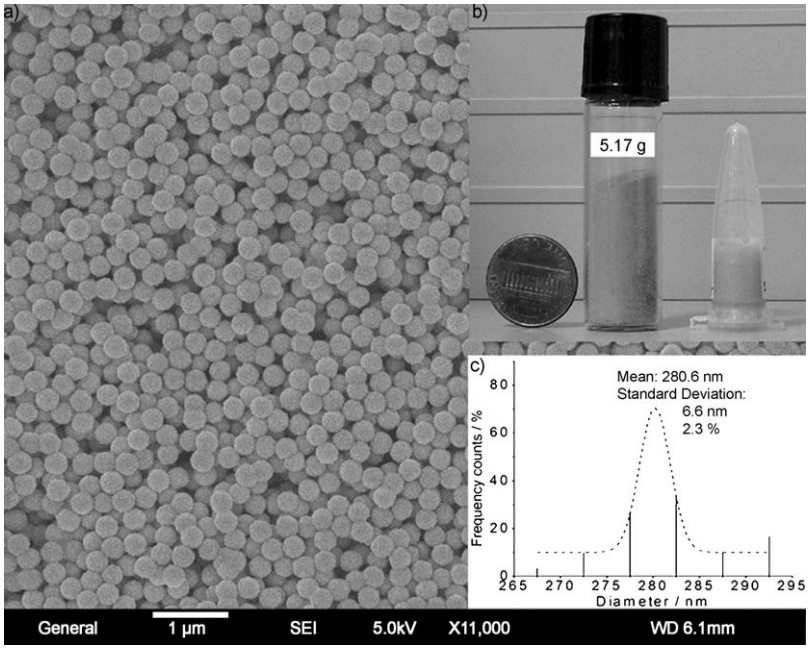

Figure 4. a) SEM image, b) photograph and c) size distribution of CSCS synthesized on a large scale (10 times).

© 2007 Wiley-VCH Verlag GmbH & Co. KGaA, Weinheim

CSCS of 281 ± 7 nm size (standard deviation: 2.3 %) are produced without any size-sorting process. Because the synthesis involves no complex or critically-controlled processes, parallel reaction systems can be easily initiated at the same time, and therefore, the synthesis of highly uniform CSCS can be leveled up (to tens or even to hundreds of grams) to meet the requirements of practical applications.

Monitoring the formation of CSCS: The growth mechanism of CSCS has been fully elucidated on the basis of TEM and UV-visible spectroscopic results. In principle, the size and concentration of CdS nanocrystals formed under a particular reaction condition can be indicated by the peak position (usually the first absorption peak on the long wavelength side) and absorbance of the UV-visible absorption spectra of the CdS nanocrystals.[34–36] Therefore, we may monitor the crystallization and growth process of CSCS by recording the UV-visible spectra of the CSCS products obtained at various reaction times.

Figure 5 shows a series of UV-visible absorption spectra of CdS particles collected at different reaction times from a reaction system which was kept at 140 °C (prior to measurement, the as-obtained sample was directly diluted 100 times by using cold ethylene glycol). The whole growth process can be simply divided to three stages. At the first stage (60–80 min), there is no obvious change in the absorption spectra in comparison with the spectrum of the unreacted sample (0 min). Whereas at the second stage (from about 90 to 140 min), the absorption becomes stronger, and the absorption band edge red-shifts gradually. This observation indicates the gradual increase of the average particle size and concentration of the CdS nanocrystals. At the third stage (about 150 min and later), the UV-visible absorption peaks are more distinct as the CdS particles continue to grow, meanwhile no obvious increase in the average size of the primary nanocrystals was observed. After the size of the CdS spheres reaches such a value that the particle diameter matches the wavelength of ultraviolet or visible light, the absorption band edge becomes unclear because of reflection or scattering of the ultraviolet or visible light by the CdS spheres. In the meantime, the reaction solution becomes turbid as shown in Figure 6f.

Though no color change for the reaction solution and peak change for the UV-visible spectrum are observed at the first stage, CdS nanocrystals with a diameter of 5.1 ± 1.3 nm form, as shown, for example, in Figures 6a,g and S8a in the Supporting Information (reaction time: 60 min). These nanocrystals aggregate to form larger secondary particles at the second stage. The secondary "cores" or particles obtained after a reaction time of 120 min are about 23.4 ± 4.0 nm in diameter as shown in Figure 6b. The corresponding HRTEM image reveals that the nanocrystals in the "cores" are packed in such a way that the individual core appears as a single crystal (Figures 6h and S8b in the Supporting Information). The visible lattice fringes of these core particles are found to run across the whole core structure. Gaps between the primary nanocrystals do not alter

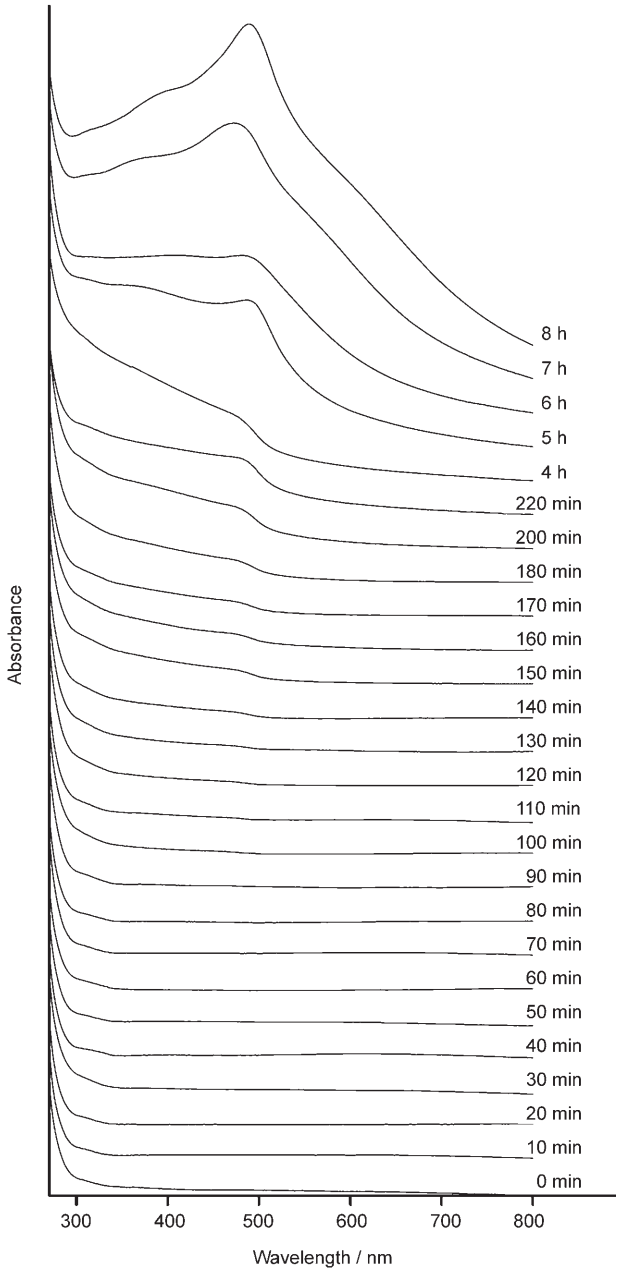

Figure 5. UV/Vis spectra of the CSCS samples collected at various reaction time intervals from 0 min to 8 h (Cd^{2+}, TU, and PVP concentrations: 0.1 M each, reaction temperature: 140 °C).

the lattice orientation. The Fast Fourier Transform (FFT) patterns of the corresponding areas in Figure 6h also prove that the core particle has a single crystalline feature, although it is composed of smaller nanocrystals. This observation indicates that the primary nanocrystals are packed to the secondary core particles through an oriented attachment route.[37–40]

Once the "cores" are formed through oriented attachment, they grow larger with reaction time at the third stage. It is intriguing to elucidate how these smaller "cores" grow. As shown in Figure 6, at the earlier stage of the process, the "cores" grow with the disappearance of most individual CdS

 © 2007 Wiley-VCH Verlag GmbH & Co. KGaA, Weinheim

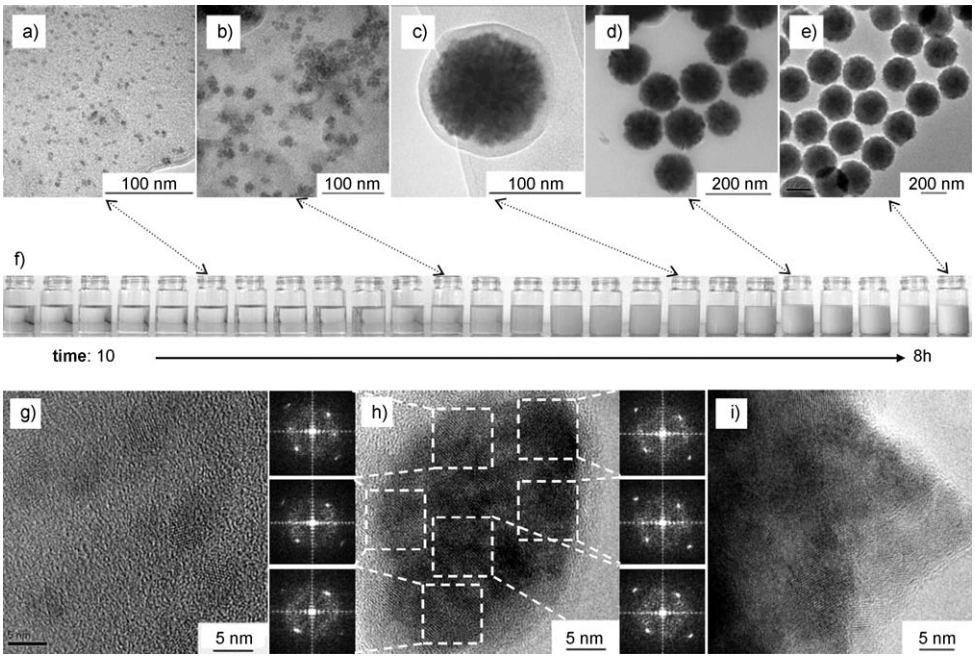

Figure 6. Evolution of size and morphology of CSCS obtained at 140 °C (Cd^{2+}, TU, and PVP concentrations: 0.1 M each): TEM images of CSCS collected at a reaction time of: a) 1 h; b) 2 h; c) 3 h; d) 4 h; and e) 8 h; HRTEM images of the corresponding particles collected at: g) 1 h; h) 2 h; and i) 8 h. The photograph of all samples collected at 10 min to 8 h is presented in (f). The images attached to (h) are Fast Fourier Transform (FFT) patterns, obtained by using program Image-Pro Plus 5.0, of the corresponding areas in (h).

nanocrystals. One typical HRTEM image of CdS spheres (reaction time: 8 h) is shown in Figures 6i and S8c in the Supporting Information, and it is seen that the orientations of all visible lattice fringes of the primary nanocrystals are random without a specific attachment axis. These nanocrystals are mostly smaller than 20 nm.

Our observation sheds light on the previous two ambiguous issues, that is, how original cores form from separated nanoparticles and how these smaller cores grow larger. In our system, the slow, but continuous formation of the small nanocrystals, the 3D-oriented attachment of these nanocrystals to form "cores", and a fast surface growth of the "cores" to form uniform colloidal spheres through in situ formation and random attachment of additional nanocrystals, constitutes the whole growth process (Scheme 1) of the CSCS. This growth process is reminiscent of the growth pathway for transition-metal nanoclusters described by Finke and co-workers.[41]

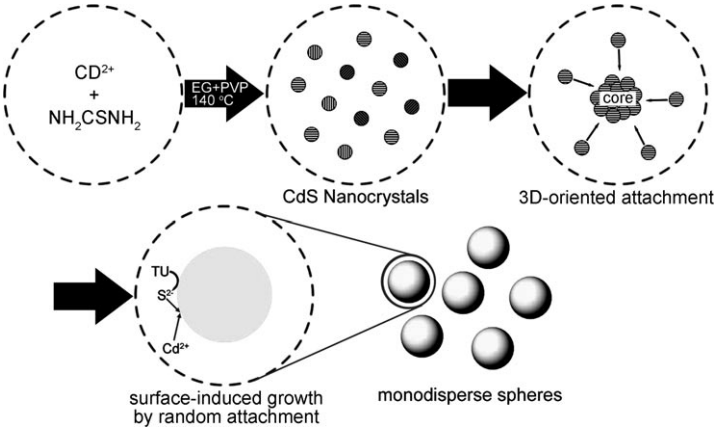

Scheme 1. Schematic representation of the growth process for CSCS.

General synthesis of noncadmium metal-sulfide colloidal spheres: The as-synthesized CSCS can be used as chemical templates for the formation of other metal-sulfide colloidal spheres which are difficult to prepare directly.[12] For example, a series of colloidal spheres (Figures 7 and 8), including Ag_2S, Bi_2S_3, Cu_2S, HgS, and Sb_2S_3 have been prepared through ion exchange of CSCS.[42]

The conversion of the spheres is preliminarily indicated by the color change of the as-obtained powder from yellow (CdS) to black (Ag_2S), brown (Bi_2S_3), dark red (Cu_2S and HgS), and orange (Sb_2S_3). The products have been identified by using X-ray diffraction (Figure 8) which also indicates the presence of residual CdS in the final colloidal spheres. In all the cases, the original CdS morphology is more or less retained except for Ag_2S with a larger size and cracked surface. Hollow spheres of HgS (Figure 7, bottom right) are obtained through removal of the CdS cores with concentrated hydrochloric acid. From the XRD pattern in combination with the TEM image of the HgS hollow spheres, it is clear that the as-synthesized HgS colloidal spheres possess a CdS/HgS core/shell structure with an amorphous HgS shell. The diameter of the metal-sulfide colloidal spheres with spherical, hollow, or core/shell structures can be tuned indirectly by varying the size of the template, CSCS. The ion-exchange

 © 2007 Wiley-VCH Verlag GmbH & Co. KGaA, Weinheim

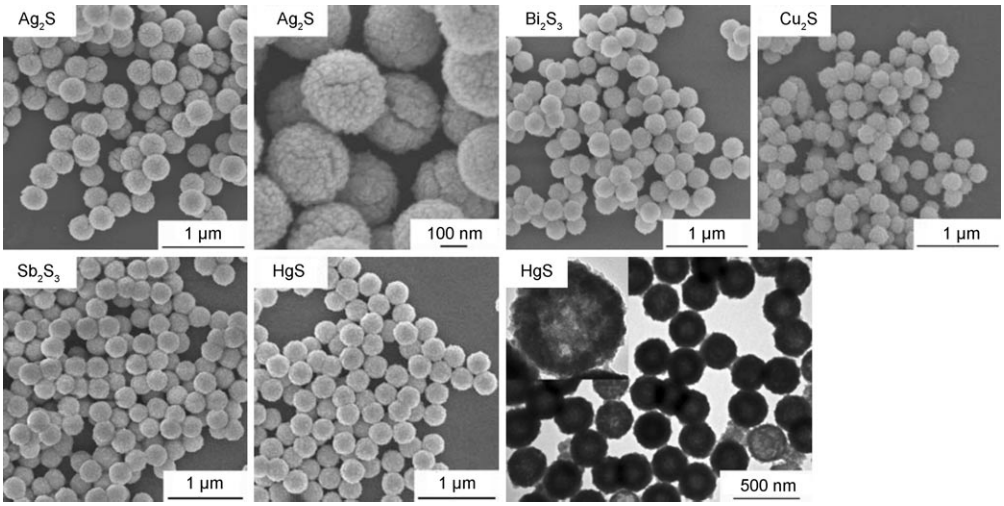

Figure 7. SEM images of the Ag_2S, Bi_2S_3, Cu_2S, Sb_2S_3, and HgS colloidal spheres and TEM image of the HgS hollow spheres obtained through the use CSCS as a template.

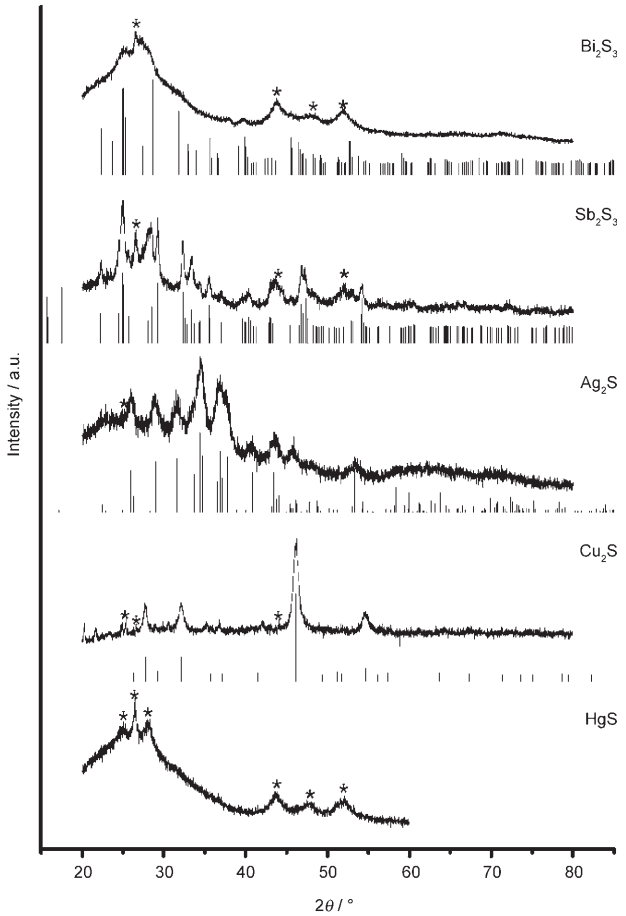

Figure 8. Powder XRD patterns of Bi_2S_3, Sb_2S_3, Ag_2S, Cu_2S, and HgS colloidal spheres. Bi_2S_3, Sb_2S_3, Ag_2S, and Cu_2S can be indexed on the basis of the standard compounds JCPDS 84-0279 (orthorhombic), JCPDS 42-1393 (orthorhombic), JCPDS 65-2356 (monoclinic), and JCPDS 47-1748 (rhombohedral), respectively (the standard diffraction peaks are represented by the bars under the patterns). The peaks marked with asterisks (*) are the reflections of the remaining CdS (JCPDS 80-0006) in the particles.

process involved proves to be an effective route for the preparation of highly monodisperse metal-sulfide (other than Cd) colloidal spheres, which may find applications in various areas, such as foams, pigments, and sensor fabrication.[14–17]

Assembly of CSCS to thin films and their optical properties: Because of their uniform size and shape, the CSCS may be used as suitable building blocks for the formation of photonic crystals, photonic balls, and functional films. Homogenous thin films (Figure 9a,b) have been fabricated through spin-coating of CSCS (sized at 380 and 280 nm, respectively) dispersed in volatile media.[10] Although the packing of the spheres in the two films is not perfect (Figure S9, Supporting Information), the films exhibit characteristic optical properties and stop band gaps of photonic crystals. As shown in Figure 9a, the reflected color of the film is green whereas the transmitted color is blue, and this is also confirmed by the reflectance spectrum (Figure 9c) which shows two strong reflectance peaks at 525 and 693 nm, respectively. When the size of CSCS is changed from 380 to 280 nm, the two reflectance peaks of the reflectance spectrum (Figure 9c) blue-shift to 456 and 547 nm, and the reflected and transmitted colors become yellow and orange, respectively (Figure 9b). These observations demonstrate that the CSCS have the potential to form novel colloidal crystals and to be used for optical device manufacture.

Conclusion

A facile solvothermal procedure has been developed for preparing highly monodisperse CdS colloidal spheres (CSCS) with tunable sizes (from 80 to 500 nm). These colloidal particles can be directly assembled into films which show characteristic stop band gaps of photonic crystals. By using the CSCS as a template, highly uniform Ag_2S, Bi_2S_3,

 © 2007 Wiley-VCH Verlag GmbH & Co. KGaA, Weinheim

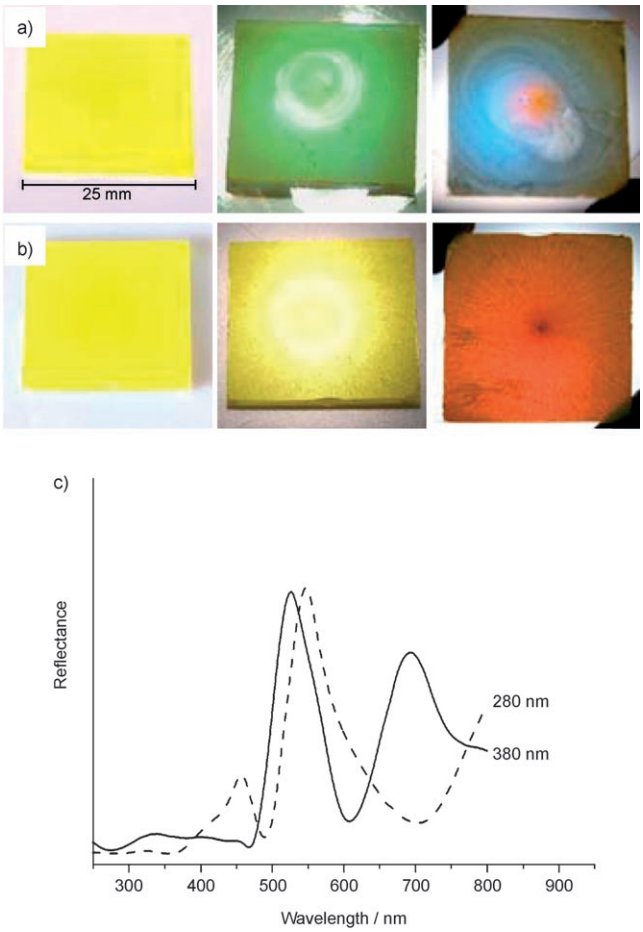

Figure 9. Photographs of the original color (left), the reflected color (middle), and the transmitted color (right) of the films composed of 380 (a) and 280 nm (b) CSCS. The corresponding reflectance spectra are shown in (c).

Cu_2S, HgS, and Sb_2S_3 colloidal spheres, which are difficult to obtain directly, have been prepared through ion exchange. We have demonstrated the mode of aggregation of the primary nanocrystals and the growth mechanism of the colloidal spheres. First, small nanocrystals are formed slowly and continuously, followed by 3D-oriented attachment of these nanocrystals to form "cores", and finally the "cores" grow to form uniform colloidal spheres through random attachment of additional nanocrystals. In principle, we are able to extend our synthetic strategy to the preparation of other colloidal spheres. For example, we have successfully synthesized monodisperse ZnS colloidal spheres and some other metal sulfide colloidal particles by using a similar method. It is expected that our synthetic approach may open new vistas for monodisperse colloidal spheres that exhibit promising physicochemical properties.

Experimental Section

Polyvinyl pyrrolidone (PVP K30, $M_W = 58000$) was purchased from BASF. Absolute ethanol, acetone, carbon tetrachloride, ethylene glycol, hydrogen peroxide, isopropyl alcohol, sulfuric acid (98 wt.%), bismuth nitrate, mercuric nitrate, silver nitrate, and thiourea (TU) were all purchased from Beijing Chemical Factory, cadmium nitrate from Shanghai Chemical Reagent Factory, tartaric acid from Northeast Pharmaceutical Factory, cuprous chloride from Tianjin No. 1 Chemical Reagent Factory, and antimony trichloride from Jiangsu Dongtai Chemical Factory. All the reagents were of analytical grade and used as received. Deionized water, high purity water (PURELAB Plus, PALL) with a resistivity of 18 MΩ cm was used throughout.

Typical synthesis of CSCS: $Cd(NO_3)_2{\cdot}3H_2O$ (1.080 g, 3.5 mmol), TU (0.266 g, 3.5 mmol), and PVP (0.389 g, 3.5 mmol, calculated in terms of the repeating unit C_6H_9NO $F_W = 111$) were dissolved in ethylene glycol (35 mL) and stirred vigorously until homogeneous. The mixture was sealed in a 50 mL PTFE-lined stainless-steel autoclave and was heated at 140 °C for 8 h followed by cooling to RT. The resulting colloidal solution was precipitated with acetone and separated by centrifugation (7000 rpm, 10 min). The yellow precipitation was further washed thoroughly with deionized water to remove all residual reagents.

Formation of M_xS (M_xS: Ag_2S, Bi_2S_3, Sb_2S_3, and HgS) colloidal spheres from CSCS: As-synthesized CSCS (0.108 g) and PVP (0.167 g, 1.5 mmol) were dispersed homogeneously in ethylene glycol (10 mL) through stirring and sonication. A solution of M_xNO_3 in ethylene glycol (20 mL) was then added to the mixture (the final concentration was 0.02 M) followed by stirring for 1–20 h (20 h for Ag_2S, Bi_2S_3, and Sb_2S_3 and 1 h for HgS). For HgS formation, the final reaction mixture was further treated at 70 °C for 4 h. The products were separated by centrifugation and washed thoroughly with deionized water to remove all residual reagents. Hollow HgS spheres were obtained through treating the CdS–HgS colloidal spheres with a 2 M solution of HCl which dissolved the unreacted CdS cores from the CdS–HgS particles.

Formation of Cu_2S colloidal spheres from CSCS: Under vigorous stirring, as-synthesized CSCS (0.108 g), tartaric acid (0.045 g, 0.3 mmol), and CuCl (0.149 g, 1.5 mmol) were successively added into deionized water (30 mL) with an interval of 10 min. The final solution was further stirred for 20 h, and the product was separated by centrifugation and washed thoroughly with deionized water to remove all residual reagents.

CSCS film preparation:[10] Glass slides were cut into squares (25×25 mm) and were washed successively with deionized water, acetone, carbon tetrachloride (ultrasonicated for 30 min), isopropyl alcohol, deionized water, piranha solution (mixed 4:1 solution of sulfuric acid and hydrogen peroxide, ultrasonicated for 1 h), and deionized water, followed by drying through blowing with nitrogen gas. These glass slides were then used as substrates for film preparation. A suspension (200 μL) containing about 10 wt.% ethanol, 40 wt.% EG, and 50 wt.% CSCS was uniformly spread on one glass substrate through tilting and rotating. The wet substrate with the suspension was dried on a homemade spin coater with a rotating speed of 6000 or 4500 rpm for 15 min.

General characterization: The UV/Vis spectra of the CSCS samples collected at various reaction time intervals from 0 min to 8 h were recorded on a Shimadzu UV-2450 spectrophotometer, and the reflectance spectra of the films at normal incidence were obtained on a Shimadzu UV-3600 spectrophotometer. The scanning electron microscopic (SEM) images were taken with a JEOL JSM 6700F electron microscope operating at 5 kV, whereas the transmission electron microscopic (TEM) and high-resolution transmission electron microscopic (HRTEM) imaging, and the energy-dispersive spectroscopy (EDS) were performed on a JEOL JEM-3010 TEM microscope equipped with an X-ray energy-dispersive spectroscopy system. The thermogravimetric and differential thermal analysis (TG/DTA) curves were recorded on a NETZSCH STA 449C TG/DTA thermal analyzer at a heating rate of 10 °C min^{-1} under nitrogen protection. The IR spectra were acquired on a Bruker IFS 66v/S FTIR spectrometer, whereas the powder X-ray diffraction (XRD) patterns were recorded on a Rigaku D/Max 2550 X-ray diffractometer by using a $Cu_{K\alpha}$ radiation ($\lambda = 1.5418$ Å).

© 2007 Wiley-VCH Verlag GmbH & Co. KGaA, Weinheim

Acknowledgement

This work was supported by the National Natural Science Foundation of China.

[1] H. J. Reiss, *J. Chem. Phys.* **1951**, *19*, 482–487.
[2] J. R. Savage, D. W. Blair, A. J. Levine, R. A. Guyer, A. D. Dinsmore, *Science* **2006**, *314*, 795–798.
[3] V. T. Manoharan, M. T. Elsesser, D. J. Pine, *Science* **2003**, *301*, 483–487.
[4] Y. Xia, B. Gates, Y. Yin, Y. Lu, *Adv. Mater.* **2000**, *12*, 693–713.
[5] E. Matijević, *Chem. Mater.* **1993**, *5*, 412–426.
[6] X. Yan, J. Yao, G. Lu, X. Chen, K. Zhang, B. Yang, *J. Am. Chem. Soc.* **2004**, *126*, 10510–10511.
[7] S. H. Park, D. Qin, Y. Xia, *Adv. Mater.* **1998**, *10*, 1028–1032.
[8] P. Jiang, J. F. Bertone, K. S. Hwang, V. L. Colvin, *Chem. Mater.* **1999**, *11*, 2132–2140.
[9] Y. Lu, Y. Yin, B. Gates, Y. Xia, *Langmuir* **2001**, *17*, 6344–6350.
[10] A. Mihi, M. Ocaña, H. Míguez, *Adv. Mater.* **2006**, *18*, 2244–2249.
[11] J. Huang, A. R. Tao, S. Connor, R. He, P. Yang, *Nano Lett.* **2006**, *6*, 524–529.
[12] U. Jeong, Y. Wang, M. Ibisate, Y. Xia, *Adv. Funct. Mater.* **2005**, *15*, 1907–1921.
[13] X. Jiang, T. Herricks, Y. Xia, *Adv. Mater.* **2003**, *15*, 1205–1209.
[14] S. Fujii, A. J. Ryan, S. P. Armes, *J. Am. Chem. Soc.* **2006**, *128*, 7882–7886.
[15] S. H. Kim, S. Y. Lee, G. R. Yi, D. J. Pine, S. M. Yang, *J. Am. Chem. Soc.* **2006**, *128*, 10897–10904.
[16] R. A. Barry, P. Wiltzius, *Langmuir* **2006**, *22*, 1369–1374.
[17] X. Zhao, Y. Cao, F. Ito, H. H. Chen, K. Nagai, Y. H. Zhao, Z. Z. Gu, *Angew. Chem.* **2006**, *118*, 6989–6992; *Angew. Chem. Int. Ed.* **2006**, *45*, 6835–6838.
[18] S. Libert, V. Gorshkov, V. Privman, D. Goia, E. Matijević, *Adv. Colloid Interface Sci.* **2003**, *100–102*, 169–183.
[19] A. Celikkaya, M. Akinc, *J. Am. Ceram. Soc.* **1990**, *73*, 2360–2365.
[20] D. M. Wilhelmy, E. Matijević, *J. Chem. Soc. Faraday Trans*, **1984**, *80*, 563–570.
[21] E. Matijević, *Langmuir* **1986**, *2*, 12–20.
[22] A. Celikkaya, M. Akinc, *J. Am. Ceram. Soc.* **1990**, *73*, 245–250.
[23] T. Sugimoto, S. Chen, *A. Muramatsu, Colloids Surf. A.* **1998**, *135*, 207–226.
[24] K. P. Velikov, A. van Blaaderen, *Langmuir* **2001**, *17*, 4779–4786.
[25] Q. Wu, H. Cao, S. Zhang, X. Zhang, D. Rabinovich, *Inorg. Chem.* **2006**, *45*, 7316–7322.
[26] S. Xiong, B. Xi, C. Wang, G. Zou, L. Fei, W. Wang, Y. Qian, *Chem. Eur. J.* **2007**, *13*, 3076–3081.
[27] J. Huang, Y. Xie, B. Li, Y. Liu, Y. Qian, S. Zhang, *Adv. Mater.* **2000**, *12*, 808–811.
[28] P. C. Rieke, S. B. Bentjen, *Chem. Mater.* **1993**, *5*, 43–53.
[29] M. L. Breen, J. T. Woodward, D. K. Schwartz, *Chem. Mater.* **1998**, *10*, 710–717.
[30] J. Yang, J. H. Zeng, S. H. Yu, Y. Li, G. E. Zhou, Y. T. Qian, *Chem. Mater.* **2000**, *12*, 3259–3263.
[31] A. M. Qin, Y. P. Fang, H. D. Ou, H. Q. Liu, C. Y. Su, *Cryst. Growth Des.* **2005**, *5*, 855–860.
[32] H. Xu, W. Wang, W. Zhu, L. Zhou, *Nanotechnology* **2006**, *17*, 3649–3654.
[33] X. H. Li, D. H. Zhang, J. S. Chen, *J. Am. Chem. Soc.* **2006**, *128*, 8382–8383.
[34] C. B. Murray, D. J. Norris, M. G. Bawendi, *J. Am. Chem. Soc.* **1993**, *115*, 8706–8715.
[35] X. Peng, J. Wickman, A. P. Alivisatos, *J. Am. Chem. Soc.* **1998**, *120*, 5343–5344.
[36] L. Qu, W. Yu, X. Peng, *Nano Lett.* **2004**, *4*, 465–469.
[37] A. P. Alivisatos, *Science* **2000**, *289*, 736–737.
[38] Z. Tang, N. A. Kotov, M. Giersig, *Science* **2002**, *297*, 237–240.
[39] A. Narayanaswamy, H. Xu, N. Pradhan, M. Kim, X. Peng, *J. Am. Chem. Soc.* **2006**, *128*, 10310–10319.
[40] A. Narayanaswamy, H. Xu, N. Pradhan, X. Peng, *Angew. Chem.* **2006**, *118*, 5487–5490; *Angew. Chem. Int. Ed.* **2006**, *45*, 5361–5364.
[41] M. A. Watzky, R. G. Finke, *J. Am. Chem. Soc.* **1997**, *119*, 10382–10400.
[42] L. Dloczik, R. Könenkamp, *Nano Lett.* **2003**, *3*, 651–653.

Received: May 18, 2007
Published online: August 3, 2007

 © 2007 Wiley-VCH Verlag GmbH & Co. KGaA, Weinheim